Article

Not peer-reviewed version

Upper Limb Orthoses: Integrating Topology Optimization and 3D Printing for Custom Fit and Function

Stefanos Voulgaris , George Kazakis , Konstantinos Iason Ypsilantis , Dimitrios Galanis , Charoula Kousiatza , Chara Ch. Mitropoulou , Maria Gkara , Stelios K. Georgantzinos , Konstantinos Soultanis , Nikos D. Lagaros *

Posted Date: 1 October 2024

doi: 10.20944/preprints202410.0049.v1

Keywords: Topology optimization; personalized wrist braces; 3D printing; 3D scanning; computer-aided design; additive manufacturing

 doi:10.20944/preprints202410.0049.v1

Article

Upper Limb Orthoses: Integrating Topology Optimization and 3D Printing for Custom Fit and Function

Stefanos Voulgaris [1,†], George Kazakis [1,†], Konstantinos-Iason Ypsilantis [2,†], Dimitrios Galanis [3,†], Charoula Kousiatza [4,†], Chara Ch. Mitropoulou [5,†], Maria Gkara [6,†], Stelios K. Georgantzinos [7,†], Konstantinos Soultanis [3,†] and Nikos D. Lagaros [1,†,*]

[1] Department of Structural Engineering, Institute of Structural Analysis and Antiseismic Research, School of Civil Engineering, National Technical University Athens, Heroon Polytechniou Str. 9, Zografou Campus, 15780, Athens, Greece WWW home page: http://users.ntua.gr/nlagaros
[2] KU Leuven, Department of Mechanical Engineering, Div. LMSD, Jan De Nayerlaan 5, 2860, Sint-Katelijne-Waver, Belgium.
[3] First Department of Orthopaedics, Attiko Hospital, School of Medicine, National and Kapodistrian University of Athens, Athens, Greece.
[4] Akmelogi S.M.P.C., Idras Str. 8, Dafni, 17237, Athens, Greece.
[5] Infersence LTD, Agiou Sosti Str., 32300, Orchomenos, Viotia, Greece.
[6] Innovasphere LTD, Stara planina Str. 80, 1527, Sofia, Bulgaria.
[7] Department of Aerospace Science and Technology, National and Kapodistrian University of Athens, 34400 Psachna, Greece.
* Correspondence: nlagaros@central.ntua.gr
† These authors contributed equally to this work.

Abstract: Customized wrist splints, particularly for upper extremity orthoses like wrist support braces, are commonly used across numerous clinical scenarios. However, the traditional process for producing personalized wrist splints is largely manual and highly dependent on the expertise of orthopedic specialists. This experience-based approach often leads to suboptimal outcomes, necessitating further refinement of the designs. Recent advancements in Additive Manufacturing (AM) have brought significant innovation to various industries, including orthopedics. This study aims to present a comprehensive methodology that integrates advanced design tools ,like 3D Scanning, with digital manufacturing techniques to produce tailored wrist splints. The produced hand brace aims to offer enhanced mechanical performance and comfort by precisely fitting an individual's anatomy while minimizing material usage and weight. To achieve optimal design efficiency, the study explores the application of a Topology Optimization (TO) approach for design, while the manufacturing process utilizes Fused Deposition Modeling (FDM), an evolving technology within the Additive Manufacturing (AM) sector.

Keywords: Topology optimization; personalized wrist braces; 3D printing; 3D scanning; computer-aided design; additive manufacturing

1. Introduction

Hand casts have long been a standard treatment for fractures, supporting and immobilizing the injured area to ensure proper healing [1]. While effective in stabilizing bone injuries, traditional plaster or fiberglass casts come with a set of drawbacks. They are often heavy limit the wearer's mobility. Additionally, their non-breathable material can trap moisture against the skin, leading to discomfort, itching, and skin infections. The inability to remove the cast complicates the monitoring of the healing process and personal hygiene, making them less than ideal for long-term recovery [2,3]. To solve these setbacks, a new type of brace is suggested using recent advances in manufacturing technology.

Over the past few years, additive manufacturing (AM) has made significant strides in various fields, including orthopedic medicine. As a result, there has been a growing body of research on creating personalized orthopedic braces using such a technology [4–11]. For instance, Ronca et al [8] studied the different materials that can be used for 3D printing orthopedic scoliosis braces, while Zhhang et al. proposed a randomised controlled trial to determine the clinical effectiveness of 3D printed braces versus thoracolumbosacral orthoses for patients with Adolescent idiopathic scoliosis.

 doi:10.20944/preprints202410.0049.v1

All these studies have demonstrated significant advancements in this area, with various materials and design methodologies being explored to improve the functionality and comfort of orthopedic braces. However, the existing research has primarily relied on the expertise and design intuition of the researcher or designer, This approach might not always lead to an optimized solution, especially for complex problems such as the development of personalized orthoses, that require specific design goals while operating under various constraints.

In this study, we leverage the application of TO techniques to create optimized designs for orthopedic devices, where several published studies have explored similar topics and have provided valuable insights [12–16]. TO is employed to address the challenge of designing a splint that can withstand specific boundary conditions while minimizing weight and maximizing strength. Additionally, the functional and aesthetic aspects of the splint, as well as the patient's hygiene and comfort, are taken into consideration during the design process. To achieve the desired outcome, the proposed process utilizes numerical analysis methods such as the Finite Element Method (FEM), along with an optimization algorithm that accounts for various criteria and constraints. The initial design domain, required by the optimization problem, is generated using Computer-Aided Design (CAD) tools, which are based on 3D scans of the patient's hand anatomy obtained through modern scanning technologies.

This study showcases the efficiency of an approach that integrates TO with AM technologies for designing and producing personalized orthoses for the upper limb. In comparison to wrist splints that are designed and fabricated through traditional means, the proposed methodology provides superior comfort, ease of use, and hygiene, while producing orthotic designs that are lighter and adequately strong. Moreover, this approach shows promise in treating a broader range of clinical cases beyond wrist fractures and in creating different types of orthoses, including those for the lower limb and spine.

2. Topology Optimization and Problem Formulation

The formulation of a typical optimization problem comprises three essential elements [17,18]: (i) a vector of input data (known as design variables) that describe all potential system designs, (ii) one or more objective functions that establish the system's criteria for assessing the efficiency of each design, and (iii) a set of constraint functions that determine the feasibility of each design. After formulating the optimization problem, the objective of the optimization process is to identify the combination of the design variables that optimizes the objective functions to the greatest extent possible, while also satisfying the constraints.

The general formulation of an optimization problem can be expressed mathematically with the following Equation 1:

$$\begin{aligned} & min_x f(x) \\ & s.t. \\ & g_j(x) \leq 0,\ j = 1, 2, ..., m \\ & h_k(x) = 0,\ k = 1, 2, ..., p \\ & x = [x_i],\ i = 1, 2, ..., n\ x_{i,lower} \leq x_i \leq x_{i,upper} \end{aligned} \tag{1}$$

where $f(x)$ is the objective function to be optimized (minimized or maximized depending on the problem), $g_j(x)$ and $h_k(x)$ represent the inequality and equality constraint functions, respectively, and the vector x specifies the design variables. The design variables x are set up to configure the objective function $f(x)$, ensuring they adhere to the constraints $g(x)$ and $h(x)$. The parameters $x_{i,lower}$ and $x_{i,upper}$ represent the minimum and maximum thresholds of the vector x, respectively, while the subscripts j and k indicate the count of inequality and equality constraints, respectively.

 doi:10.20944/preprints202410.0049.v1

A standard TO problem can be formulated as follows:

$$\begin{aligned} & C(x) = F^T \cdot U(x) \\ & s.t. \\ & F = K \cdot U(x) \\ & V(x)/V_0 = f \\ & 0 \leq x_e \leq 1 \quad \ldots e = 1 : n_e \end{aligned} \tag{2}$$

where the structural compliance value $C(x)$ is the objective function to be minimized, vector F encompasses the external forces applied, and $U(x)$ refers to the displacement vectors calculated by solving the structural equilibrium equation $F = K \cdot U(x)$. The variables $V(x)$ and V_0 represent the volume of the structure and the total domain volume, respectively, while n_e specifies the number of finite elements (FEs) used to discretize the structure. The target volume percentage is symbolized by f, and x_e indicates the material density for element e.

In general, TO can be considered as the procedure of optimally distributing a specified material volume inside a specific design domain in order to transfer the loading conditions to the structural supports. The change in the material distribution is achieved by removing or adding material to areas of the design domain [19].

In contrast to sizing and shape optimization formulations which utilize dimensions or coordinates as design variables, TO introduces a new artificial quantity that defines the existence or absence of material within each FE, so-called relative material density. Thus, in the TO problem the optimization algorithm mainly uses the material densities to indicate the existence of parts of the domain in order to achieve the final solution. The solution of the TO problem follows the Solid Isotropic Microstructure with Penalization for intermediate densities (SIMP) method [20–22]. SIMP is a gradient-based method based on a continuously converging algorithm, which is controlled by a penalization parameter, p. In the original design domain, each FE of the discretized initial section corresponds to a design variable, which is generally thought of as the relative element density, ρ_e. This relative density in each element is related to the modulus of elasticity, E_e, based on the following equation:

$$E_e = (\rho_e)^p E_0 \tag{3}$$

where E_0 is the initial modulus of elasticity of the element in the solid phase corresponding to $\rho = 1$, E_e is the new "artificial" modulus of elasticity of element number e and the parameter p is the penalty factor that the more it increases, the more it reduces the yield of intermediate density elements and forces the design to be close to a $0/1$ (void/solid) solution. A typical value of the penalty factor for plates and shell structures is $p = 2$ and for solids it is $p \geq 3$. Prior to addressing a TO problem, it is important to adhere to a series of steps to ensure accurate problem formulation [13,23,24]: (1) Development of the TO problem, (2) Collection of the necessary data and information, (3) Define the design variables, (4) Select the criterion to be optimized, and (5) constraint functions. In this study the design steps are expressed through the following two stages followed by the manufacturing stage: (1) generating the design domain and formulation of FE model, (2) selection of the objective and constraint functions, and then the solution stage of the TO problem.

3. Generating the Design Domain and the Associated FE Model

To serve as the foundation for the TO process, a 3D model of the wrist brace must be produced. This starts with generating a 3D model of the patient's arm with the use of a 3D scanner, which will then be used to design the necessary wrist brace. Through 3D Scanning, the digital representation of the complex anatomical features of a specific person's hand-wrist limb is achieved, which then forms the basis for the development of the initial model of the personalized wrist splint, through the application of a series of computational design software (CAD).

 doi:10.20944/preprints202410.0049.v1

3.1. 3D Scanning Feature

For the digital representation of the human anatomy, there are nowadays various methods that can be used, e.g. Computed Tomography - CT, Magnetic Tomography (Magnetic Resonance Imaging - MRI), as well as 3D Scanning technology. Both Axial and Magnetic tomography offer the possibility of digital representation even of the internal parts of the human anatomy with quite high precision. For the creation of personalized orthoses, the digital representation of the internal morphology of the human anatomy is most of the times not necessary, depending on the anatomic area of interest, and for this reason the constantly evolving 3D Scanning technology plays an important role in this field, as it enables the visualization of only the external surfaces, thus reducing to greatly both the data to be obtained and the time to process it to render the final digital model.

Similar to the methods of Axial and Magnetic Tomography, the 3D Scanning technology also presents some disadvantages, which include the inability of receiving data with great accuracy on the surfaces of the anatomy characterized by quite complex geometric features (e.g. areas between the fingers on the extreme hand), resulting in either gaps or unwanted convergence of points in the corresponding areas, thus making it necessary to further process the obtained data in order to repair the final model. In addition, another drawback is the presence of noise in the final model due to possible movement of the anatomy during the scanning process, thus necessitating, usually, the use of special custom supports at specific points to avoid unintended movement.

In this research, the scanning was performed using the EinScan-SE 3D Scanner by Shining 3D® Tech Co., Hangzhou, China [25]. During the scanning process, the hand was positioned neutrally, aligned at 0° relative to the two motion axes, with the fingers in a relaxed state resembling the grip on a glass (see Figure 1). This posture facilitated the capture of data in the less visible regions, primarily located between the fingers. The result of each scanned surface, from the whole anatomy of the studied hand, was visible in real time during the scanning process. It is important to note that for optimal connection of the individual scanned surfaces of the hand to create the final model of the hand, the design of some "guide" points on it was done hand, which were quite distinct from the 3D Scanner. The hand remained stationary during the process of scanning each surface, and was then moved in such a way as to obtain data from the remaining parts of the anatomy as necessary. Stabilization of the arm is deemed necessary in order to obtain a good digital model representation of the actual anatomy. For this reason, the use of some supports (Figure 1) was deemed necessary after the first scanning tests, as after the first minutes of the procedure it was difficult to control the position, as well as the standstill of the arm. The whole process took about 15 minutes after the first tests were carried out, mainly due to the inability to completely immobilize the hand and the great complexity of the surface to be scanned.

 doi:10.20944/preprints202410.0049.v1

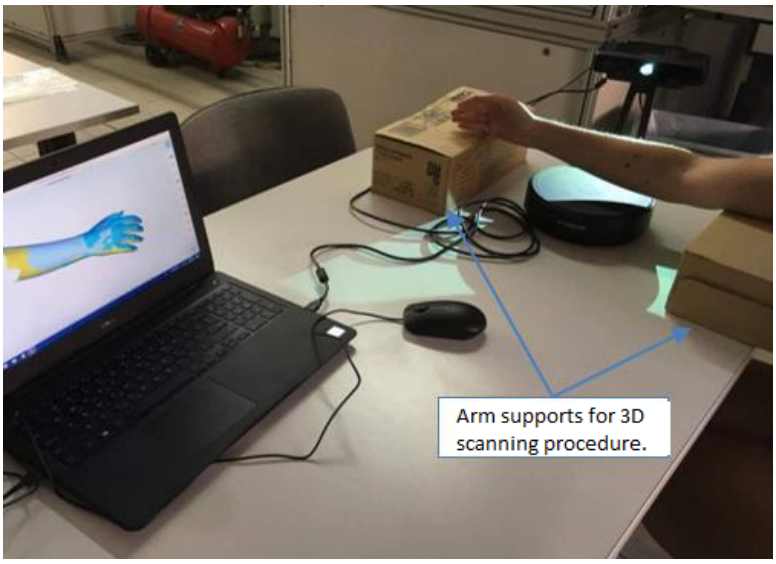

Figure 1. 3D Scanning Procedure: The arm is supported and the hand was positioned neutrally with the fingers in a relaxed state

3.2. Post Processing and Designing the Brace

With the completion of the 3D scanning process, the 3D model of each patient's hand (in this work of the healthy author's hand) is recovered, which includes all the anatomical features that are different for each person. This model forms the basis in the developed methodology, to create the original personalized wrist brace, which is then optimized by applying the TO method. The digital model needs to undergo further processing, as mentioned above, in order to reduce the "noise" and eliminate the small imperfections that have arisen. To create the initial model of the wrist splint, CAD software are used. Specificaly: MeshMixer (Autodesk), Geomagic Design X (3D Systems) and SolidWorks (Dassault Systèmes). Using the software Meshmixer the scanned arm model was manually repaired and modified to produce the personalized wrist brace.

The repair process included the following important processes: elimination of data that constitutes "noise" for the hand model, reshaping and filling of discontinuities mainly in the areas of the fingers as well as in a small part of the forearm, smoothing the outer surface in various places, as well as reducing the number of mesh polygons to reduce the file size, which is necessary to undergo further modeling. The reduction in the number of mesh polygons was such that it did not affect the final result, in terms of the representative representation of real anatomy details.

The step-by-step repair of the hand model performed in the Meshmixer [26] software is shown in Figure 2. In blue color are depicted the imperfections of the model in the initial stages of repair, while in light gray color is shown the final model that resulted after the completion of this process.

 doi:10.20944/preprints202410.0049.v1

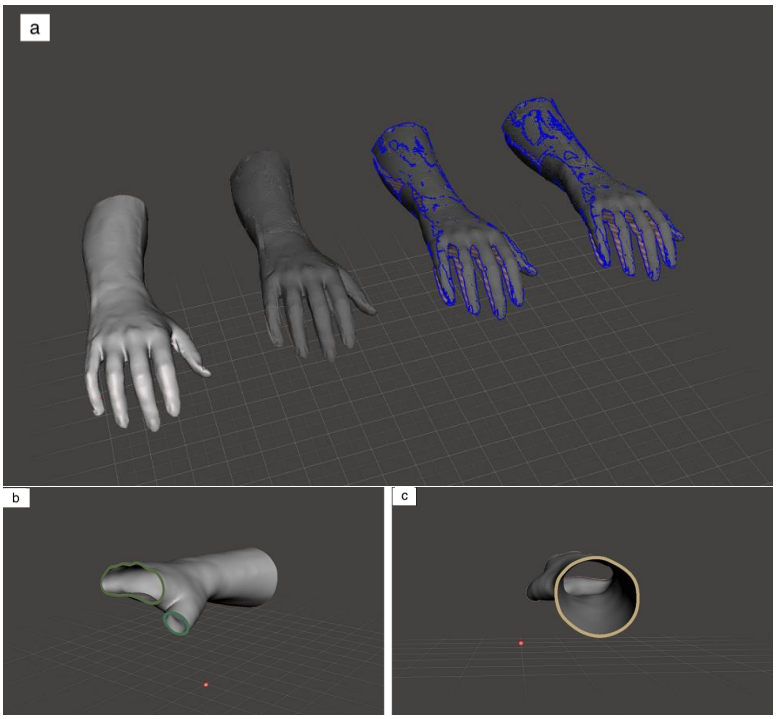

Figure 2. a) Repairing the 3D hand model, from right to left, remove seperate meshes (noise), fill holes, smooth mesh imperfections. b) Removal of the fingers. c) Expanding the model by 1mm and offsetting it outwards by 3mm.

After completing the repair of the hand model, the next stage of the proposed methodology is the development of an initial design of a personalized wrist splint, on which the TO problem will be solved. Part of this process is done in the MeshMixer software. First, it is necessary to make such processing of the hand model, so that the design of the resulting splint meets the basic geometric specifications of such an orthoses. For this purpose it is necessary to remove parts of the anatomy that are not needed which include part of the forearm as well as the areas of the fingers, thus ensuring their full movement (Figure 2). Then, the outer surface of the specific geometry is shifted outwards by 1 mm, in order to achieve the patient's complete comfort during the application of the splint and to avoid the creation of wounds due to pressure, especially on the bony protrusion of the forearm and the hand. The resulting final surface is subsequently transformed into a fully solid structure 3 mm thick, which is shown in Figure 2, by offsetting the shifted surface 3mm outwards.

Using Geomagic Design X software (3D Systems, Rock Hill, South Carolina, USA), the model is converted to a CAD model through the ability to gives the auto surfacing tool. Figure 3 shows the CAD models resulting from the creation of a denser and a thinner mesh of splines, respectively, which define the final surface of each model. The wrist splint model consisting of the sparsest mesh with splines is the one selected for further processing in the design package SolidWorks (Dassault Systèmes, Vélizy-Villacoublay, France), in order to create a much lighter computational model for the TO process.

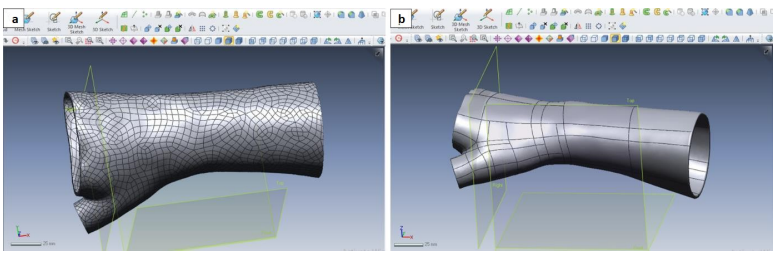

Figure 3. CAD models of the wrist splint resulting from creating a) a denser and b) a sparser mesh of splines in Geomagic Design X.

 doi:10.20944/preprints202410.0049.v1

The parametric design of the wrist splint model was carried out in SolidWorks. In particular, a plane was designed along the model based on which the adaptation will be separated into two pieces for convenience during its application, as well as two planes of intersection at the two ends (Figure 4a), in order for the splint to satisfy the necessary design and ergonomic criteria, while also taking into account the limitation of dimensions that can be manufactured on the printing platform of the available 3D printers. In addition, some splines are designed (Figure 4b-c) at certain distances from the two ends (15 mm from the forearm side and 30 mm from the finger side), as well as from the middle plane (7.5 mm), which through the split line command will lead to the creation of the design and non-design areas in the splint model. These areas, as discussed below, play a very important role in how to solve the TO problem. The model of the customized wrist brace obtained through the parametric design in SolidWorks and illustrated in Figure 4, is saved in Initial Graphics Exchange Specification file format (.iges) and is the basis of which the TO problem is solved.

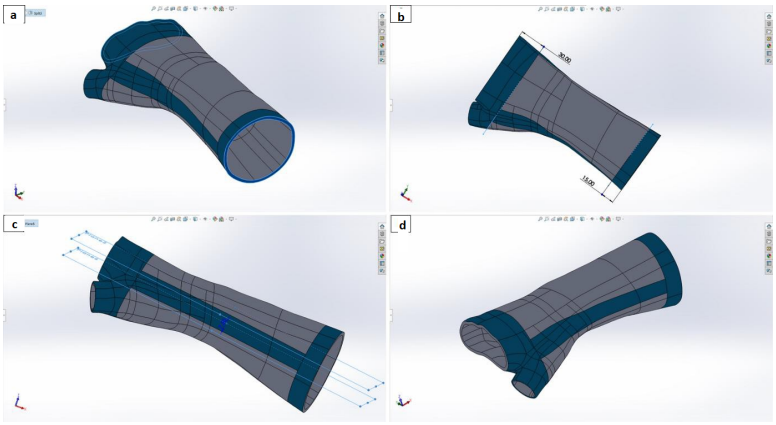

Figure 4. Parametric design of the wrist splint model. (a) Incision at both ends (forearm and fingers), (b) Designing splines at a distance of 15 mm on the forearm side and 30 mm on the finger side, (c) Creation of a plane along the model and splines at a distance of 7.5 mm from the middle plane and (d) Final model of customized wrist splint based on which the TO problem is solved.

3.3. Design Domain

The design domain refers to the section of the model where material can be removed during the TO process to achieve the optimal design. In contrast, the non-design domain is the area that remains unaltered because it is typically essential for connecting to other parts and components. In the creation of the wrist splint model, the structure was divided into two categories: "free" and "fixed," using HyperMesh, a software tool within Hyperworks® 14.0 [27]. The "free" areas, designated as the design domain, are subjected to mesh optimization, allowing for material removal to optimize the design. Meanwhile, the "fixed" areas, designated as the non-design domain, remain unchanged (Figure 5).

Using HyperMesh for this subdivision facilitates precise control over which parts of the wrist splint can be modified during the TO process. The clear distinction between the design and non-design domains ensures that critical structural and functional components of the splint remain intact while allowing for significant weight reduction and performance improvement in the free areas. This approach balances optimization efficiency with practical considerations, resulting in a robust and functional final design.

 doi:10.20944/preprints202410.0049.v1

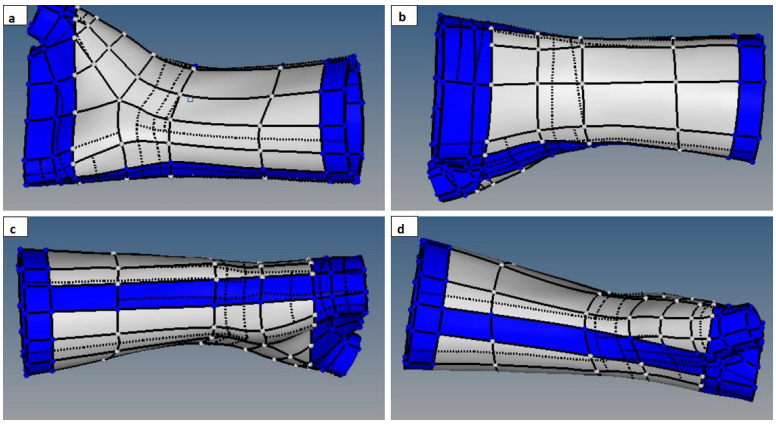

Figure 5. The "fixed" areas are depicted in blue, whereas the "free" are shown in white. Views: a) Palmar view, b) Dorsal view, c) View from the ulnar side, d) View from the radial side.

3.4. Developing the FE Model

Once the design domain has been established, several crucial steps must be completed to advance the design process. These steps include: (1) *Mesh Generation:* This involves discretizing the design domain into a finite number of elements to facilitate numerical analysis. (2) *Determination of Material Properties:* In this stage, the physical and mechanical properties of the materials used in the design are defined, which is essential for accurate simulation results. (3) *Determination of Load Cases:* This step involves specifying the types and magnitudes of loads that will be applied to the design, reflecting the real-world conditions the final product will encounter. Each of these stages is critical for ensuring that the design process is thorough and that the final optimized model meets the required performance criteria. Detailed explanations of these stages are provided in the subsequent sections:

3.4.1. Mesh Generation

Mesh generation was conducted using HyperMesh, resulting in the creation of three distinct models. Each model is constructed from 4-node tetrahedral elements. The first two models were designed for the first and second load cases, respectively, with the primary difference being their mesh densities. The third model, intended for the third load case, is similar to the second in terms of mesh density. The first model features a coarse mesh, with element sizes of 1.5 mm, comprising 211,422 elements and 56,168 nodes. In contrast, the second and third models employ a finer mesh, with element sizes of 1 mm. This higher node density results in each model containing 668088 elements and 157395 nodes (Figure 6).

Using HyperMesh allows for precise control over mesh density, which is crucial for accurately simulating different load cases. The coarse mesh of the first model provides a broad approximation, suitable for initial analyses where computational efficiency is a priority. However, the fine meshes of the second and third models offer greater detail and accuracy, essential for more refined and precise simulations. This differentiation ensures that the models can adequately capture the structural responses under varying conditions, enhancing the reliability and validity of the simulation results.

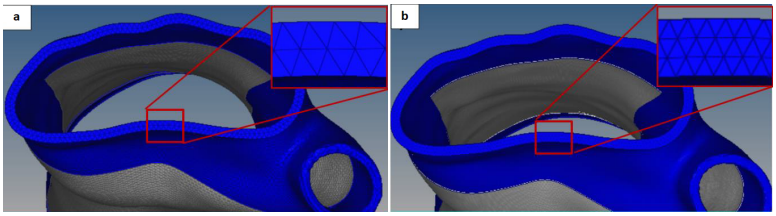

Figure 6. a) Coarse mesh with 1.5 mm element size and b) Fine mesh with 1.0 mm element size applied to the case of wrist deviation and flexion.

 doi:10.20944/preprints202410.0049.v1

Another approach regarding the discretization of the section could be the use of shell elements (2.5D shell elements), choosing either the inner or the outer surface of the splint and considering a constant thickness of 3 mm, i.e. equal to thickness of the structure. This methodology would lead to a smaller number of FEs and would decrease the computational time to solve the TO problem. This method was followed to solve a similar problem in Rossetos et al.[10] study.

3.4.2. Determination of Material Properties

As outlined in the introduction, the optimized results will be fabricated using a Fused Deposition Modeling (FDM) 3D printer. This process employs an extruded thermoplastic filament made of ABS (Acrylonitrile Butadiene Styrene). The material properties of ABS are specified as follows: Young's modulus $E = 2.2\ GPa$, Poisson's ratio $\nu = 0.35$, and Density $\rho = 1040\ kg/m^3$.

Using an FDM 3D printer offers several advantages, including the ability to produce complex geometries with relative ease and the flexibility to iterate designs rapidly. ABS is a popular choice for FDM due to its strength, durability, and good thermal stability, making it suitable for a wide range of applications. The Young's modulus indicates the stiffness of the ABS material, while the Poisson's ratio provides insight into the material's deformation characteristics under stress. The density is crucial for understanding the weight and buoyancy aspects of the printed parts.

Furthermore, conducting tensile tests on the printed specimens allows for a more precise characterization of the mechanical properties, considering the potential variations introduced during the printing process, such as layer adhesion and orientation. This experimental validation ensures that the theoretical properties align closely with the actual performance of the 3D printed parts, thereby enhancing the reliability and predictability of the final product. A tensile testing method was examined by Rossetos et al.[10].

3.4.3. Determination of Loads Cases

This investigation focuses on wrist braces intended to support the healing process of fractures located at the distal end of the radius. To replicate the forces acting on the brace precisely, two key load cases were established: radial deviation and wrist flexion. These scenarios are based on the forces applied to the brace during common wrist activities, encompassing radial and ulnar deviations, along with wrist flexion and extension, as outlined in previous studies [28] (refer to Table 1 and Figure 7a,b). The maximum forces for these load cases were estimated based on torque values reported in the literature [28]. These torque values were divided by 0.1 meters, the distance from the metacarpophalangeal joints to the wrist, to calculate the maximum forces applicable to a sample of 50 healthy individuals without hand or wrist pathologies.

Table 1. Loads cases and Constraints by Vanswearingen[28]

Load Cases	Radial Deviation	Wrist Flexion
Turning Force (Nm)	11.33	14.81
Study Forces 10% (N)	11.33	14.81
Applied Force Direction	-Y axis	-Z axis

 doi:10.20944/preprints202410.0049.v1

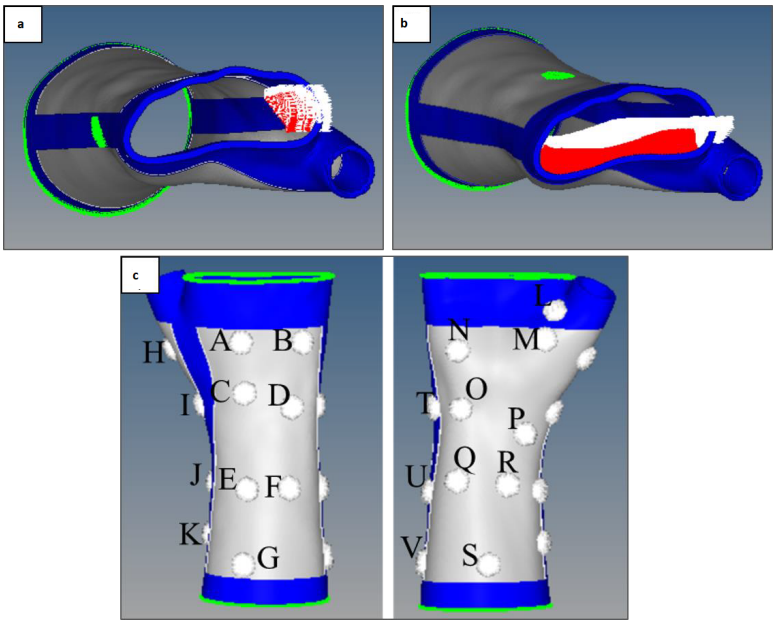

Figure 7. Load cases and constraints applied on each researched case: a) Radial Deviation, b) Wrist Flexion, c) 22 Point Forces (The green color represents the constraints)

However, it is crucial to recognize that patients with distal radius fractures typically cannot exert maximum forces due to factors such as pain and swelling. Therefore, for this study, the FE analysis was conducted using loads that are 10% of the maximum isometric forces achievable by healthy individuals. This adjustment ensures that the simulation more accurately reflects the reduced forces experienced by patients in real-world scenarios, as outlined in Table 1. In the FE model of the wrist brace, forces were applied to the areas of the brace most likely to encounter these loads during wrist movements (see Figure 7a,b). This approach aims to closely mimic actual loading conditions and ensure that the simulation results effectively represent the realistic stress and strain on the wrist brace structure.

The forces applied by the hand-wrist to the splint were quantified using specialized pressure sensors, each with a thickness of 0.20 mm, as detailed by [15]. These sensors measured forces at 22 distinct points on the splint. The force magnitudes at each of these 22 points are summarized in Table 2. It is essential to note that these forces were applied perpendicular to the relevant surfaces of the FE model, as illustrated in Figure 7c. This method ensures that the simulated loading conditions closely reflect the actual forces experienced by the splint, enhancing the accuracy of the model.

 doi:10.20944/preprints202410.0049.v1

Table 2. Loads Case 3 by Yan et al.[15]

Points on brace surface	Forces applied (N)
A	34.77 ±0.24
B	13.42 ±0.01
C	18.91 ±0.07
D	90.28 ±0.12
E	48.19 ±0.08
F	34.16 ±0.01
G	54.29 ±0.27
H	68.32 ±0.56
I	86.01 ±0.51
J	73.81 ±0.07
K	95.16 ±0.13
L	31.72 ±0.08
M	73.81 ±0.09
N	92.11 ±0.29
O	3.66 ±0.01
P	63.44 ±0.27
Q	34.16 ±0.02
R	53.07 ±0.02
S	39.04 ±0.18
T	48.19 ±0.21
U	32.94 ±0.04
V	26.84 ±0.02

In the first two load cases, the forearm is assumed to be at rest, while the upper arm and wrist are free to move but limited due to the application of the splint. This means on the back surface of the splint, all 6 degrees of freedom are bound. A second restriction is also applied for these cases to the middle of each surface of each splint model, creating a three-point applied force system so that the interactions that are simulated between the brace and the hand-wrist represent as much as possible the real ones. Accordingly, in the third load case that is studied, it is assumed that the surface of the splint at both the rear and front ends is at rest, so in the corresponding areas, all 6 degrees of freedom are bound, while a load is applied to the middle of each surface of the model at various points along and around the structure, simulating the forces that develop when applying a splint.

It is important to note that in all three load cases studied in the present work, the two individual pieces of the brace, which arise in stage of the manufacturing process are considered to be fully connected. Therefore, the FE model does not include any bounds on the surfaces where these pieces are connected.

4. Design Process for Custom Limb Orthoses

The design of custom limb orthoses is fundamentally driven by the Topology Optimization (TO) process, which involves two critical phases: formulation and solution. *Formulation Phase:* This initial phase focuses on defining the mathematical framework for the optimization problem. It involves specifying the objective function and the constraints that guide the design process. The objective function typically aims to minimize strain energy or weighted compliance, which is inversely related to the stiffness of the orthosis. By minimizing this function, the design process seeks to maximize the structural performance and stability of the orthosis. *Solution Phase:* In this phase, the TO algorithm applies the defined objective and constraints to iteratively refine the design. The process adjusts the material distribution within the orthosis to find an optimal configuration that adheres to the constraints while achieving the minimal strain energy. The constraints usually include limitations on material volume or density, ensuring that the final design is both practical to manufacture and effective in performance. The culmination of these phases results in a custom limb orthosis that is optimized for both structural efficiency and functionality, meeting the specific needs of the user while adhering to the

 doi:10.20944/preprints202410.0049.v1

practical constraints of manufacturing and material use. This approach ensures that the final product not only provides the necessary support and comfort but also utilizes materials in an efficient and cost-effective manner.

4.1. Framework: Determination of Objective and Constraint Functions

In the optimization of the wrist brace, the primary objective function employed is the deformation energy, which is also known as weighted compliance. Compliance (C) is a measure of how much a structure deforms under applied forces, and it is inversely related to the structure's stiffness (K). Thus, by minimizing the strain energy, we effectively maximize the stiffness of the wrist brace, resulting in a more robust and supportive design. To ensure that the optimization process yields a feasible and practical design, several constraints are applied. This study imposes constraints on the reduction of the initial volume fraction of the brace material, specifying reductions to 25% and 50% of the original volume. These constraints guide the optimization process to balance material usage with structural performance. The topology optimization (TO) problem is solved using an iterative approach where the volume fraction is progressively reduced. This iterative process involves updating the design in each iteration to achieve a structure that is as lightweight as possible while still meeting the imposed volume constraints. The aim is to converge to an optimal design that maximizes stiffness and performance while minimizing material usage and weight. This methodology ensures that the final wrist brace design is not only efficient in terms of material but also meets the required functional and structural performance criteria.

4.2. Addressing the TO Problem

The software used for the TO iterations is HyperWorks. In Figure 8 are presented all the TO analyses that were completed in this research. The results obtained from solving each TO problem are then processed in HyperView. In each optimized wrist brace design elements are generated that have a relative density, $0.01 \leq \rho \leq 1$. A way to visualize, understand and compare the results is to choose to display the elements that have a relative density value above some threshold. In this study, the value of the relative density that has been chosen as a limit is 0.5. This means that all elements presented in the design section (depicted in gray Figures 14 and 15) of the topologically optimized wrist splints, have a relative density value greater than or equal to 0.5 to 1 ($0.5 \leq \rho \leq 1$). All elements with density less than 0.5 have been removed in the post-processing stage in HyperView.

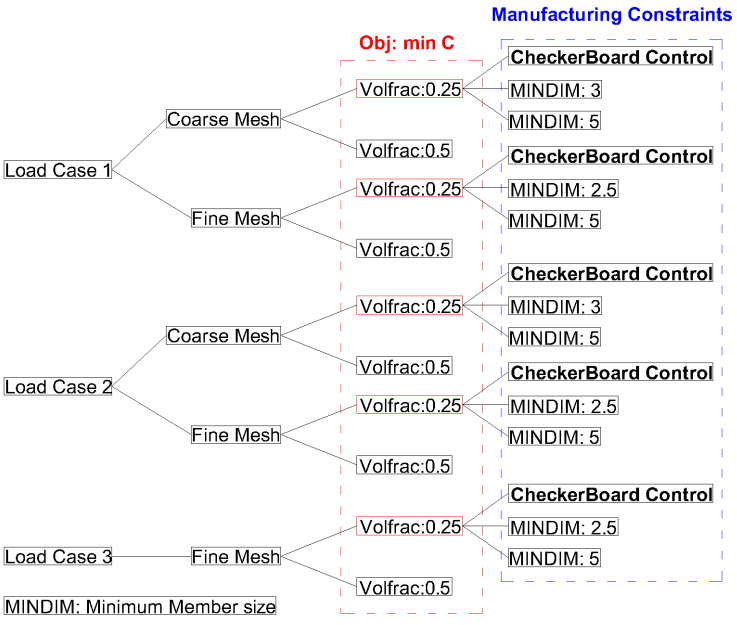

Figure 8. Topology Optimization Solutions

 doi:10.20944/preprints202410.0049.v1

In the first two load cases, regarding the radial deviation and wrist flexion, in which the effect of the discretization of the mesh (Coarse and Fine FE mesh) on the final optimal models of the splints is studied, it is observed that a finer mesh gives the final optimal designs more detail, while also leading to fewer imperfections/discontinuities in areas where a lot of material is removed. On the other hand, much faster computations can be achieved by creating a coarser mesh. This is not directly related to the number of iterations, which remain almost the same for both the fine and coarse FE meshes, however, this particular observation emerges based on the computational time each analysis takes.

Solving the TO problem determined above without applying any more constraints leads to wrist brace models with design flaws with elements that are scattered in the design space and are not connected at all to neighboring elements, thus creating several non-optimal microstructures, which are not easily implementable in construction (Figure 9).

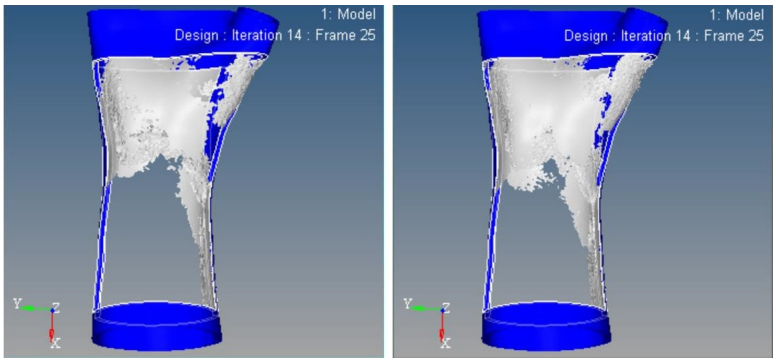

Figure 9. Wrist brace model with design flaws.

4.3. Manufacturing Constraints

The purpose of applying manufacturing constraints is to ensure that the final designs of wrist splints are optimized for easy and efficient production using 3D printing technology. This approach aims to enhance the structural integrity and geometric accuracy of the braces while simultaneously minimizing both production costs and construction time. To achieve these goals, two specific methods were employed: a) *Checkerboard Control:* This method helps prevent the formation of unwanted checkerboard patterns that can occur in additive manufacturing, ensuring a smoother and more continuous structure. b) *Minimum Member Size Control (MINDIM):* This constraint specifies the smallest allowable size for structural components, ensuring that the design is feasible for 3D printing and maintains mechanical strength. By integrating these constraints, the design process ensures that the wrist braces are both manufacturable and effective, leading to high-quality, cost-efficient, and timely production outcomes.

4.3.1. Checkerboard Control

A common problem that arises in TO of continuous structures, particularly when using first-order FEs, is checkerboarding, which is formed by alternating elements with density 1 and elements with density 0. It has been shown to be caused by errors in the FE structure and is linked to the dependence of the solution on the computational grid. This phenomenon results in the alteration of the final solution through the appearance of non-optimal microstructures (computational noise), which lead to a reduction in manufacturability. To suppress this phenomenon, by achieving solutions that are independent of the discretization of the mesh, the main techniques used are the perimeter control method, the mesh independent filtering and the density slope control.

4.3.2. Minimum Member Size Control - MINDIM

The parameter MINDIM is used to ensure that designs are both discrete and manufacturable, by defining the minimal acceptable dimensions for structural elements ([12,15,16]). As illustrated in Figure 8, the MINDIM values chosen for each analysis vary. In the case of coarse meshes, the MINDIM

 doi:10.20944/preprints202410.0049.v1

values span from 2.5 to 10.1. For fine meshes, they fall within the range of 1.7 to 6.9 [27]. Figures 10, 11, 12 compare the results of non-use, and the implementation of Checkerboard control (CHECKER) and Minimum Member Size Control (MINDIM) for splint models with coarse and fine FE mesh.

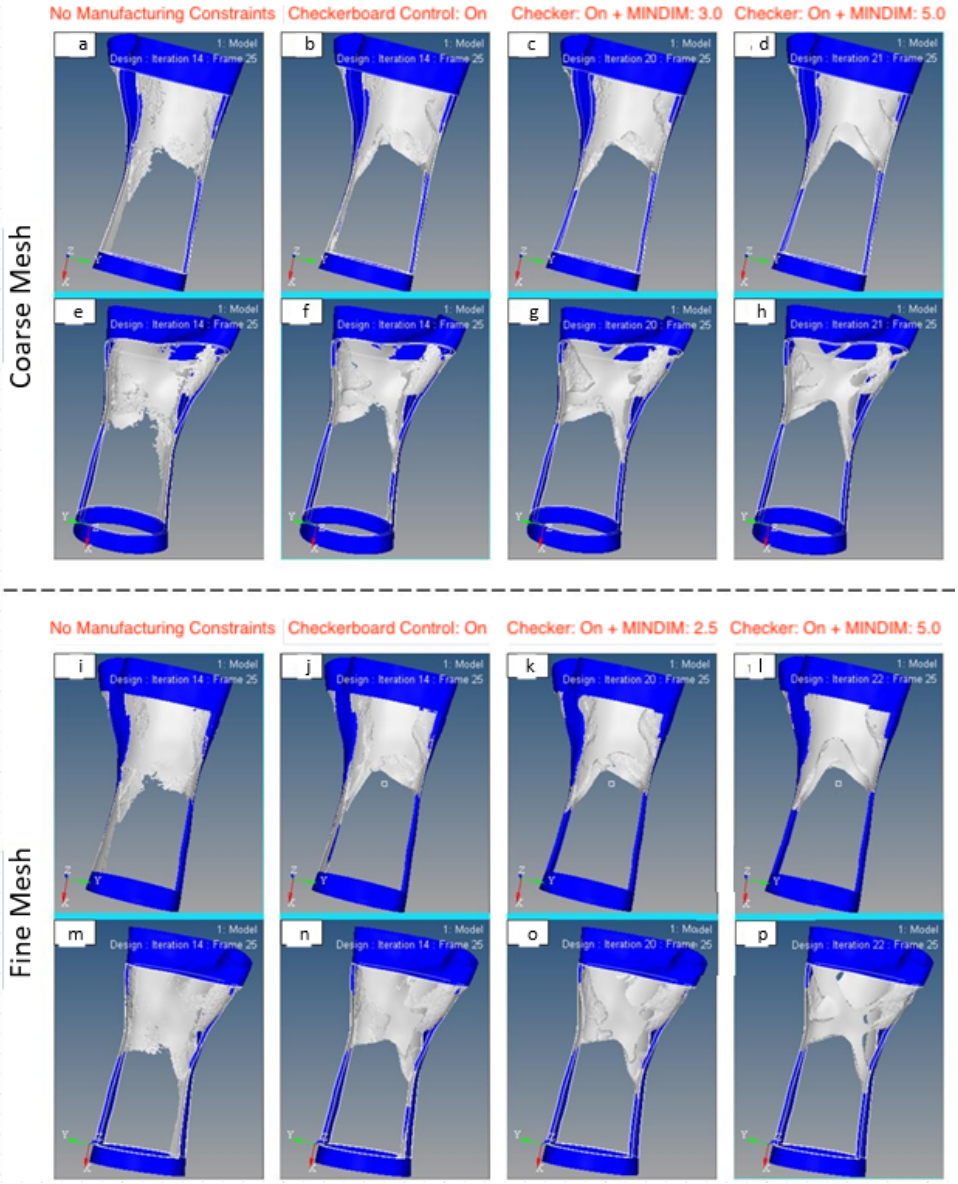

Figure 10. Load Case 1. Volfrac 25%. Comparison of results of not using, as well as applying the CHECKER and MINDIM parameters to the splint models with (a-h) the coarse and (i-p) the fine FE mesh

 doi:10.20944/preprints202410.0049.v1

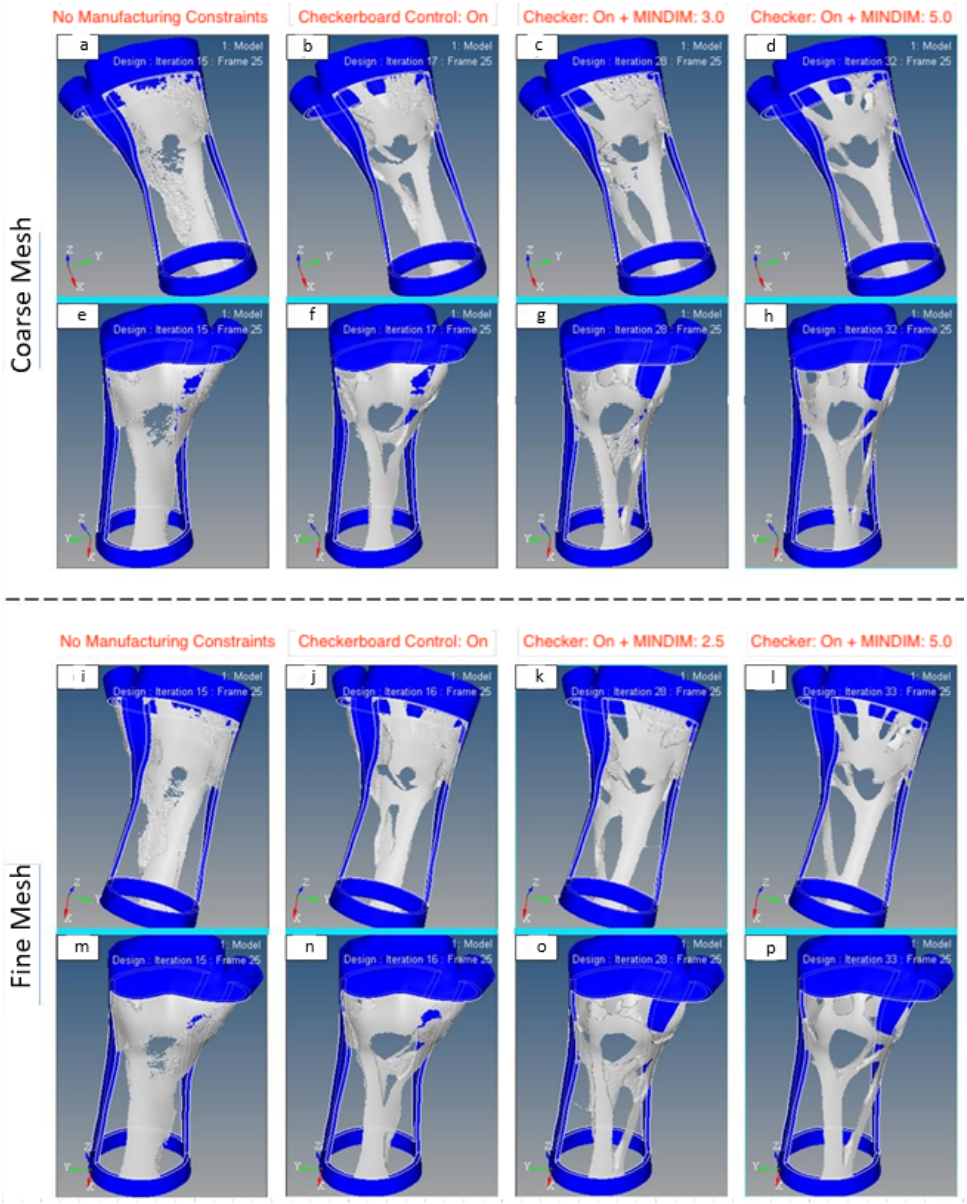

Figure 11. Load Case 2. Volfrac 25%. Comparison of results of not using, as well as applying the CHECKER and MINDIM parameters to the splint models with (a-h) the coarse and (i-p) the fine FE mesh

 doi:10.20944/preprints202410.0049.v1

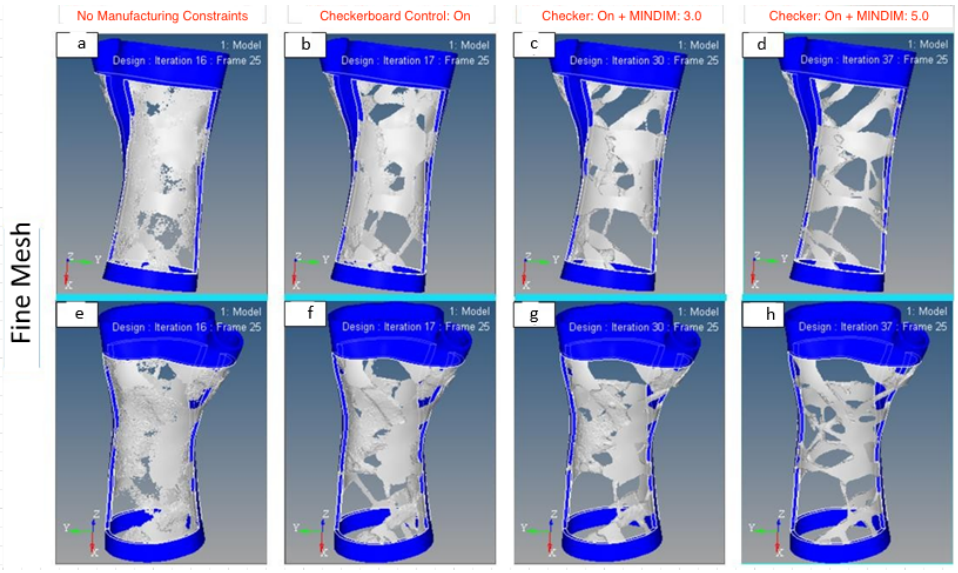

Figure 12. Load Case 3. Volfrac 25%. Comparison of results of not using, as well as applying the CHECKER and MINDIM parameters to the splint models with (a-h) the fine FE mesh

It is important to mention that applying the MINDIM constraint automatically activates the CHECKER parameter, while additionally increasing the value of the $DISCRETE$ parameter from 1 to 2. The $DISCRETE$ parameter essentially represents the penalty factor, p mentioned in Section 2, used to penalize the intermediate density elements in each design, in order to produce more distinct solutions, which are easy to manufacture. The DISCRETE parameter in Optistruct is related to the penalty factor, p, as follows: $DISCRETE = p - 1$. Therefore, in the case where the DISCRETE parameter takes the value 2, when the MINDIM constraint is applied, this means that: $p = 3$, which is a typical value of the penalty factor for solids.

Also, applying the MINDIM constraint automatically increases the number of maximum iterations that can be performed until convergence is achieved in the solution of the TO problem. The default value is 30, and the maximum number of iterations is automatically increased to 80 when the MINDIM parameter is used.

From the results of the optimal designs presented in Figures 10–12 it is observed that the application of the additional CHECKER parameter as well as the MINDIM constraint gradually leads to more distinct solutions. These solutions, especially in the case of a combined application of the two aforementioned parameters, simultaneously setting a higher value (equal to 5.0) to the MINDIM parameter, are structurally easier to implement through the 3D printing technology. For the first two load cases studied (radial deviation and wrist flexion) it is observed that the use of the denser FE mesh plays an important role in achieving wrist splint designs, which are characterized by more discrete structural members, and in particular when the denser grid is combined with the application of constraints to control the checkerboard distribution and to reduce elements with intermediate density. Another observation based on these results is that the application of the aforementioned constraints results in an increase in the number of iterations until convergence is achieved in the solution for each TO problem, nevertheless the final optimal designs of the wrist braces are design-wise and manufacturability-wise much better compared to those in which the above restrictions were not applied.

The topologically optimized wrist splints illustrated in Figures 10l,p, 11l,p and 12d,h exhibit several advantages over classically constructed splints that are widely used for the treatment of metacarpal fractures. The material removed from the original models, which based on the results of this work is observed to reach 25% of the original volume, leads to final designs of wrist splints that are considerably lighter, while at the same time exhibiting high strength. The creation of the holes in specific patterns that follow the paths of the loads for each case being studied, increases the levels of aesthetics, while in addition it enables sufficient ventilation and cleaning of the hand.

 doi:10.20944/preprints202410.0049.v1

It is important to mention that the maximum displacements based on the FE analysis for the optimal designs shown in Figures 10l,p and 11l,p are 0.077 mm and 0.286 mm, respectively, while the maximum displacement for the wrist splint design of Figure 12d,h is 0.693 mm. None of these values exceed the maximum allowed displacement limit, which is 2.5 mm for a medical splint according to the literature [15].

5. 3D Printed Results

The personalized wrist braces are manufactured using FDM technology. This particular manufacturing process is one of the most promising and widespread of those belonging to the AM technology family, due to its relatively simple operating principle, as well as the wide range of materials and machinery, which are commercially available at a fairly low cost.

5.1. Non-Optimized Brace

Printing the original non-optimized model of the wrist brace was deemed necessary mainly to avoid errors and to verify that the final geometry of the splint is fully compatible with the anatomy of the hand, before moving forward to address the TO problem based on the specific design. To create the initial design/prototype of the brace (not optimized), the Dimension Elite printer (Stratasys, Eden Prairie, MN, USA) was used, using ABS P430 (Acrylonitrile Butadiene Styrene) thermoplastic filament to create the main structure and soluble filament P400SR for the construction of the supporting structures (supports). These structures are the result of printing extra material on top of this basic model to hold the deposited material of the main structure in place, especially in areas of high geometric complexity, as it is initially in a semi-liquid state until it cools down. and solidifies completely. The prototype of the original non-optimized wrist brace design created through the use of the FDM 3D printer presented a full fit to the patient's hand while allowing finger movement to perform daily activities. Offsetting the initial scanned surface of the hand anatomy outward by 1 mm, in the design development stage, played a very important role in achieving a comfortable and at the same time stable brace model for complete immobilization of the necessary parts of the hand and freedom of movement of some others. As this model was considered quite good in terms of comfort and application, the solution to the TO problem was based on this specific wrist splint design (Figure 13).

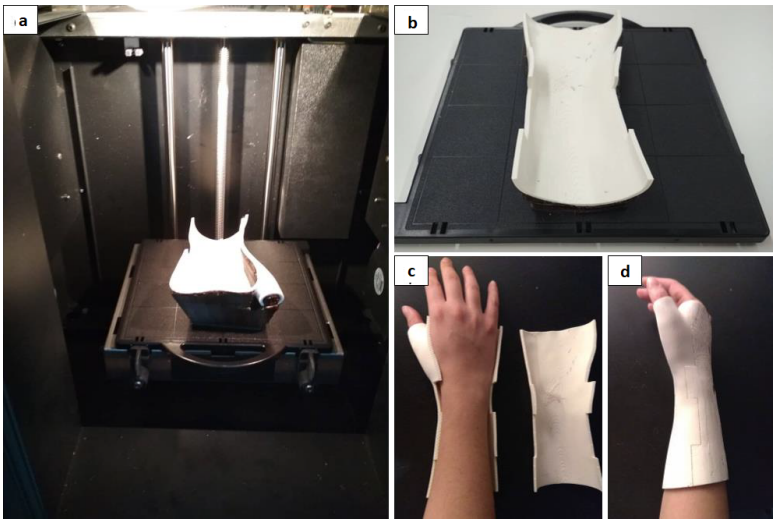

Figure 13. Fusion Deposition Modeling of the original non-optimized wrist brace design using the Stratasys Dimension Elite 3D printer. (a) Lower and (b) upper subpart of the splint, (c)-(d) complete and comfortable fit of the wrist brace prototype on the patient's hand.

 doi:10.20944/preprints202410.0049.v1

5.2. Post Processing

As the final models of the wrist braces resulting from solving the TO problem show several areas with sharp changes in their geometric characteristics, due to the removal of a lot of material from the original geometries, an important stage that intervenes before the manufacturing process is that of smoothing surface of the final designs. The purpose of this specific process is to reduce the roughness in various areas of the structure (smoothing), so that the final models of the wrist braces are characterized by structural integrity and high precision in terms of their geometric characteristics, while at the same time offering high levels of comfort during their application. This process was performed in the MeshMixer software. The models were then split into two parts (bottom and top) in the Rhino 5.0 design package environment. Each of the two individual pieces were printed separately.

5.3. Optimized Braces

It is noted that of the three load cases studied in this work, two models were constructed, based on Figures 11l,p and 12d,h: a) Wrist Flexion Brace and b) 22 Point Forces Brace (Figure 16). In the fabrication of the two optimized wrist braces, the Creator 3 3D printer [29] was utilized, using ABS filament and HIPS (High Impact Polystyrene) as the soluble filament for constructing support structures. To simplify the printing process, each wrist brace was segmented into two sections. The printing duration for each brace was 22 hours. The first 3D model was produced from the analysis that applied the second load case (Wrist Flexion) and utilized a fine mesh with a MINDIM setting of 5 (see Figure 14). The second 3D model was produced from the analysis that applied the third load case (22 Point Forces), with a fine mesh and a MINDIM parameter set to 5 (see Figure 15). Upon application, both braces match the anatomical structure of the patient's hand, offering comfort and efficient air circulation to the arm ([30]) (refer to Figure 16).

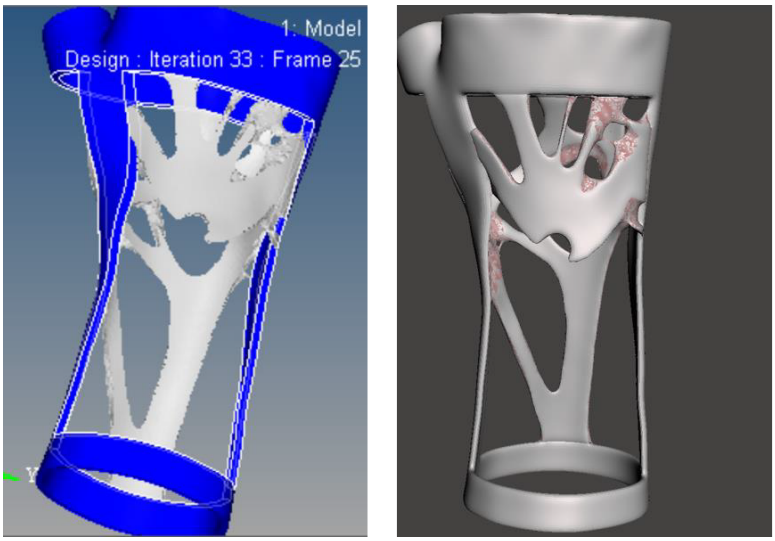

Figure 14. Optimized Brace 1 (Wrist Flexion)

 doi:10.20944/preprints202410.0049.v1

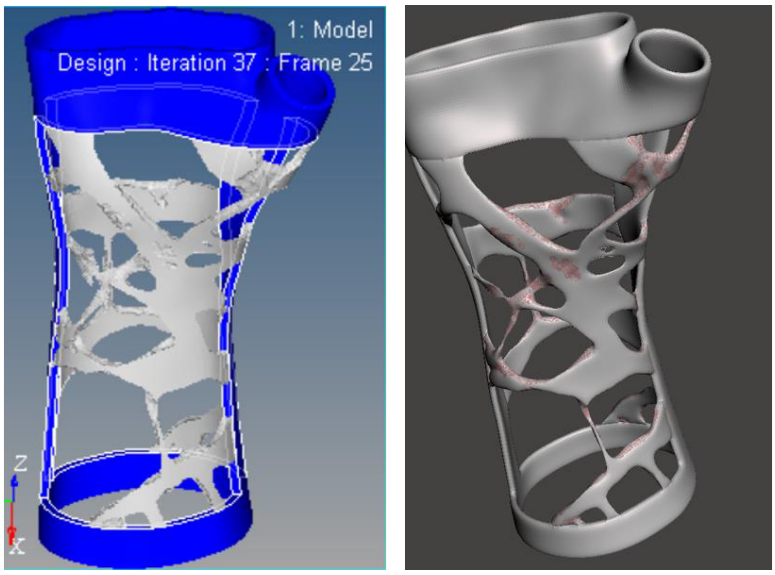

Figure 15. Optimized Wrist Brace 2 with 22-Point Force Distribution

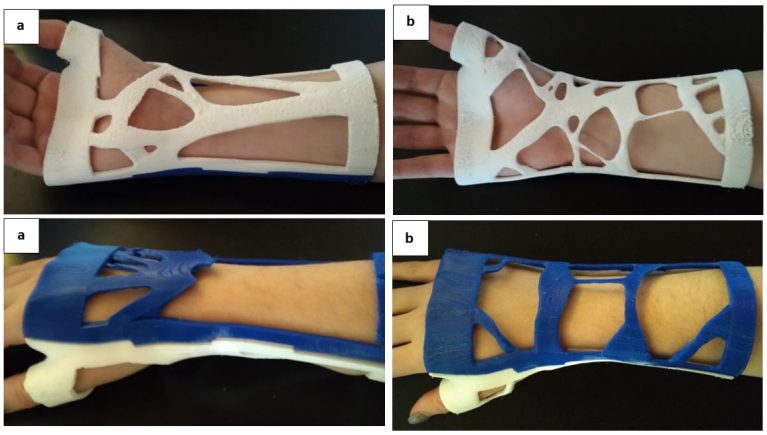

Figure 16. Customized Optimized Wrist Braces: a) Wrist Flexion Support Brace, b) 22-Point Force Distribution Brace

The parameters used for 3D printing are presented in Table 3.

Table 3. 3D Printer Parameters

3D Printer	Stratasys Dimension Elite	FlashForge Creator 3
Layer Height	0.254mm	0.2mm
Filament Deposition Angle	$\pm 45^{/circ}$	$\pm 45^{/circ}$
Printing Temperature	$270^{\circ}C$	$240^{\circ}C$
Chamber Temperature	$75^{\circ}C$	-
Infill Pattern	Rectangular	Rectangular
Infill Density	100%	100%
External Perimeters	1	1
Support Pattern	Rectangular	Tree Form

 doi:10.20944/preprints202410.0049.v1

6. Discussion

To avoid using patient data and causing discomfort during the prototype creation, we used the wrist of one of the co-authors as a reference for the design and manufacturing of the personalized wrist brace. This approach allowed us to develop the personalized wrist splint without compromising patient privacy and comfort.

The findings of this study demonstrate that combining topology optimization (TO) with additive manufacturing (AM) technology presents a promising strategy for designing and producing personalized wrist splints. However, certain practical factors must be carefully considered to ensure the effective application of this approach.

One such issue is the scanning procedure of the injured hand, which due to swelling may change shape and may later on cause discomfort. To address this, it is suggested that the 3D splint be applied at a later point in time, once the conventional cast/resin has been in place for 2-4 weeks. This will allow for more accurate scanning and the ability to continue with a 3D brace for 1-2 months. It may also be worthwhile to scan the hand while in a cast to obtain accurate information about the 3 pressure points, as researched by [31], although this may be challenging due to the thickness of the cast and coating.

The process also needs to be automated to guarantee the fast production of the 3D printed brace ensuring a smooth transition between a conventional brace (2-4 weeks) and the 3D printed one. An optimization of the printing procedure is required to minimize further the time needed to provide the brace to the patient.

Several limitations from the used material were also found during the conduct of this study. ABS can be used to demonstrate a proof of concept, but it comes with the following limitations: i) Poor 3D printing performance; ii) degradation from UV radiation and moisture absorption; iii) poor surface finish; iv) toxic fumes from 3D printing procedures; v) poor sustainability. These limitations make the choice of ABS unacceptable considering the release of a 3D-printed brace to the general public. Our next research step will consider different materials, such as polycarbonate (PETG) and nylon, as well as composite materials produced by our recycling machine.

Finally, the waterproof construction of the 3D wrist brace may have significant implications for the treatment of simple fractures and tendonitis in children and adults, as it can make daily application easier, more comfortable, and more effective. Further research in this area may be warranted to explore the potential benefits of this approach for a wider range of clinical cases.

7. Conclusion

From the solution of the TO problem, it is clear that both the density of the mesh and the constraints related to manufacturing significantly influenced the development of the optimized final models. Additionally, it would be valuable to investigate the integration of the three load cases, each with a defined influence rate, into the TO process. This approach aims to generate a wrist splint model that is better suited for accommodating average wrist movements.

The wrist braces manufactured are characterized by excellent accuracy, as even areas of the orthoses with high geometric complexity appear to be fully created without any parts collapsing. This is due both to the printing direction of the two individual pieces of each brace on the printer platform, and to the smoothing process of the structural members carried out before the 3D printing. It is important to note that despite the possibility of printing, to a very satisfactory degree, the possibility of failure of the delicate structural members is possible during the conduct of daily activities. Therefore, the further study of the specific design is deemed necessary. From the application of the braces, it is observed that the models meet the criteria of compatibility with the anatomy of the patient's hand, as well as comfort, proper ventilation of the skin and good aesthetics. It is also important to mention that in both the first and second optimized wrist brace prototypes, which were manufactured through the FDM technique, it is necessary to thoroughly study the optimal way of connecting the two individual pieces at the level of future research. The methods utilized in this study have the potential for further

 doi:10.20944/preprints202410.0049.v1

refinement and can be adapted for application in a variety of clinical cases and across different types of orthotic devices.

Author Contributions: Conceptualization, N.D.L., G.K. and C.K.; methodology, S.K.G., D.G. and K.S.; software, S.V., G.K. and K.I.Y.; validation, N.D.L., S.K.G. and K.S.; formal analysis, S.V. and K.I.Y.; investigation, C.C.M., G.K. and K.I.Y.; resources, N.D.L.; data curation, M.G., D.G. and C.K.; writing—original draft preparation, S.V.; writing—review and editing, G.K., K.I.Y., D.G., C.C.M., M.G., S.K.G., K.S. and N.D.L.; visualization, S.V. and N.D.L.; supervision, N.D.L.; project administration, N.D.L.; funding acquisition, N.D.L..
All authors have read and agreed to the published version of the manuscript.

Funding: This research has been supported by the OrThOP3Dics project: "Topology optimization of 3D printed patient-specific spinal braces" (No: TAEDK-06191) belonging to the National Recovery and Resilience Plan, Greece 2.0 Project.

Informed Consent Statement: The co-author was fully informed of the study's purpose and methodology, and provided her explicit consent for the use of her wrist as a reference.

Data Availability Statement:

- Availability of data and materials: Not applicable
- Code availability: Not applicable

Acknowledgments: This research has been supported by the OrThOP3Dics project: "Topology optimization of 3D printed patient-specific spinal braces" (No: TAEDK-06191) belonging to the National Recovery and Resilience Plan, Greece 2.0 Project.

Conflicts of Interest: The authors declare no conflict of interest.

Abbreviations

The following abbreviations are used in this manuscript:

AM	Additive Manufacturing
TO	Topology Optimization
FEM	Finite Element Method
SIMP	Solid Isotropic Microstructure with Penalization for intermediate densities
CAD	Computer-Aided Design
FDM	Fused Deposition Modeling
FE	Finite Element

References

1. KARANTANA, A.; DOWNS-WHEELER, M.J.; WEBB, K.; PEARCE, C.A.; JOHNSON, A.; BANNISTER, G.C. The Effects of Scaphoid and Colles Casts on Hand Function. *Journal of Hand Surgery* **2006**, *31*, 436–438. Publisher: SAGE Publications, doi:10.1016/J.JHSB.2006.03.163.
2. Dadkhah-Tehrani, M.; Adib-Hajbaghery, M.; Abedi, A. Frequency of cast-related complications and influencing factors in patients with casts. *International Journal of Orthopaedic and Trauma Nursing* **2022**, *46*, 100955. doi:10.1016/j.ijotn.2022.100955.
3. Drake, D.F.; Ritzman, T.F. Cast-Related Complications. *Orthopedic Clinics* **2021**, *52*, 231–240. Publisher: Elsevier, doi:10.1016/j.ocl.2021.03.005.
4. Mavroidis, C.; Ranky, R.G.; Sivak, M.L.; Patritti, B.L.; DiPisa, J.; Caddle, A.; Gilhooly, K.; Govoni, L.; Sivak, S.; Lancia, M.; Drillio, R.; Bonato, P. Patient specific ankle-foot orthoses using rapid prototyping. *J Neuroeng Rehabil* **2011**, *8*, 1. doi:10.1186/1743-0003-8-1.
5. Li, J.; Tanaka, H. Rapid customization system for 3D-printed splint using programmable modeling technique - a practical approach. *3D Print Med* **2018**, *4*, 5. doi:10.1186/s41205-018-0027-6.
6. Zhang, Y.; Liang, J.; Xu, N.; Zeng, L.; Du, C.; Du, Y.; Zeng, Y.; Yu, M.; Liu, Z. 3D-printed brace in the treatment of adolescent idiopathic scoliosis: a study protocol of a prospective randomised controlled trial. *BMJ Open* **2020**, *10*, e038373. Publisher: British Medical Journal Publishing Group Section: Surgery, doi:10.1136/bmjopen-2020-038373.
7. Redaelli, D.F.; Abbate, V.; Storm, F.A.; Ronca, A.; Sorrentino, A.; De Capitani, C.; Biffi, E.; Ambrosio, L.; Colombo, G.; Fraschini, P. 3D printing orthopedic scoliosis braces: a test comparing FDM with thermoforming. *Int J Adv Manuf Technol* **2020**, *111*, 1707–1720. doi:10.1007/s00170-020-06181-1.

8. Ronca, A.; Abbate, V.; Redaelli, D.F.; Storm, F.A.; Cesaro, G.; De Capitani, C.; Sorrentino, A.; Colombo, G.; Fraschini, P.; Ambrosio, L. A Comparative Study for Material Selection in 3D Printing of Scoliosis Back Brace. *Materials* **2022**, *15*, 5724. Number: 16 Publisher: Multidisciplinary Digital Publishing Institute, doi:10.3390/ma15165724.
9. Jin, H.; Zhang, Z.; Gao, Y.; He, H.; Feng, S.; Xu, R.; Li, Q.; Zuo, H. Case series: 3D printed orthopedic brace combined with traditional manipulative physiotherapy to treat new-onset scoliosis in adults. *Medicine (Baltimore)* **2022**, *101*, e28429. doi:10.1097/MD.0000000000028429.
10. Rossetos, I.; Gantes, C.J.; Kazakis, G.; Voulgaris, S.; Galanis, D.; Pliarchopoulou, F.; Soultanis, K.; Lagaros, N.D. Numerical Modeling and Nonlinear Finite Element Analysis of Conventional and 3D-Printed Spinal Braces. *Applied Sciences* **2024**, *14*, 1735. Number: 5 Publisher: Multidisciplinary Digital Publishing Institute, doi:10.3390/app14051735.
11. Rogkas, N.; Vakouftsis, C.; Spitas, V.; Lagaros, N.D.; Georgantzinos, S.K. Design Aspects of Additive Manufacturing at Microscale: A Review. *Micromachines* **2022**, *13*. doi:10.3390/mi13050775.
12. Huang, T.H.; Feng, C.K.; Gung, Y.W.; Tsai, M.W.; Chen, C.S.; Liu, C.L. Optimization design of thumbspica splint using finite element method. *Med Biol Eng Comput* **2006**, *44*, 1105–1111. doi:10.1007/s11517-006-0131-4.
13. Gebisa, A.W.; Lemu, H.G. A case study on topology optimized design for additive manufacturing. *IOP Conf. Ser.: Mater. Sci. Eng.* **2017**, *276*, 012026. doi:10.1088/1757-899X/276/1/012026.
14. Fiuk, G.; Mrzygłód, M. Topology optimization of structures with stress and additive manufacturing constraints. *Journal of Theoretical and Applied Mechanics* **2020**, *58*, 459–468. Publisher: Polskie Towarzystwo Mechaniki Teoretycznej i Stosowanej (PTMTS), doi:10.15632/jtam-pl/118899.
15. Yan, W.; Ding, M.; Kong, B.; Xi, X.; Zhou, M. Lightweight Splint Design for Individualized Treatment of Distal Radius Fracture. *J. Med. Syst.* **2019**, *43*, 1–10. doi:10.1007/s10916-019-1404-4.
16. Zhang, Y.; Kwok, T.H. Customization and topology optimization of compression casts/braces on two-manifold surfaces. *Computer-Aided Design* **2019**, *111*, 113–122. doi:10.1016/j.cad.2019.02.005.
17. Frangedaki, E.; Sardone, L.; Marano, G.C.; Lagaros, N.D. Optimisation-driven design in the architectural, engineering and construction industry. *Proceedings of the Institution of Civil Engineers - Structures and Buildings* **2023**, *176*, 998–1009, [https://doi.org/10.1680/jstbu.22.00032]. doi:10.1680/jstbu.22.00032.
18. Lagaros, N.D.; Plevris, V.; Kallioras, N.A. The Mosaic of Metaheuristic Algorithms in Structural Optimization. *Archives of Computational Methods in Engineering* **2022**, *29*, 5457–5492. doi:10.1007/s11831-022-09773-0.
19. Bendsøe, M.P.; Sigmund, O. *Topology Optimization*; Springer Berlin Heidelberg, 2004. doi:10.1007/978-3-662-05086-6.
20. Rozvany, G. *The SIMP method in topology optimization - Theoretical background, advantages and new applications*; 2000. Journal Abbreviation: 8th Symposium on Multidisciplinary Analysis and Optimization Publication Title: 8th Symposium on Multidisciplinary Analysis and Optimization, doi:10.2514/6.2000-4738.
21. Sigmund, O. Sigmund, O.: A 99 Line Topology Optimization Code Written in MATLAB. Structural and Multidisciplinary Optimization 21, 120-127. *Structural and Multidisciplinary Optimization* **2001**, *21*, 120–127. doi:10.1007/s001580050176.
22. Andreassen, E.; Clausen, A.; Schevenels, M.; Lazarov, B.; Sigmund, O. Efficient topology optimization in MATLAB using 88 lines of code. *Structural and Multidisciplinary Optimization* **2011**, *43*, 1–16. doi:10.1007/s00158-010-0594-7.
23. Bendsøe, M.P.; Kikuchi, N. Generating optimal topologies in structural design using a homogenization method. *Computer Methods in Applied Mechanics and Engineering* **1988**, *71*, 197–224. doi:10.1016/0045-7825(88)90086-2.
24. Kazakis, G.; Lagaros, N.D. Topology Optimization Based Material Design for 3D Domains Using MATLAB. *Applied Sciences* **2022**, *12*, 10902. Number: 21 Publisher: Multidisciplinary Digital Publishing Institute, doi:10.3390/app122110902.
25. EinScan. EinScan-SE Powerful Desktop 3D Scanner.
26. Meshmixer. Meshmixer by Autodesk.
27. Altair. Driving More Design with Simulation | Altair HyperWorks.
28. Vanswearingen, J.M. Measuring Wrist Muscle Strength. *J Orthop Sports Phys Ther* **1983**, *4*, 217–228. doi:10.2519/jospt.1983.4.4.217.
29. Flashforge. Flashforge Creator 3 FDM 3D Printer Large Build Volume.

 doi:10.20944/preprints202410.0049.v1

30. Webster, J.B.; Murphy, D.P. *Atlas of Orthoses and Assistive Devices - 5th Edition*; 2019.
31. Sinikumpu, J.J.; Nietosvaara, Y. Treatment of Distal Forearm Fractures in Children. *Scand J Surg* **2021**, *110*, 276–280. doi:10.1177/1457496920983104.